Characterization of clusters in rapid granular flows

R. Brent Rice and Christine M. Hrenya*
Department of Chemical and Biological Engineering, University of Colorado, Boulder, Colorado 80309, USA
(Received 2 September 2008; published 11 February 2009)

The clustering phenomenon within two-dimensional, rapid granular, simple shear flows is investigated. Two characterizations are developed and implemented for monodisperse systems, revealing physically meaningful insight. First, a new feature of the radial distribution function is identified for these dissipative granular systems, which is not present in molecular (nondissipative) systems. Namely, a *long-scale* minimum occurs at a distance representing the average distance between the center of a cluster and the center of a dilute region. Results indicate that center-to-center distances are least (i.e., clusters are most tightly packed) for systems of moderate particle concentrations and low restitution coefficients. In addition, concentration and temperature measurements of clustered and dilute regions are also obtained using a Gaussian filter that is based on this center-to-center distance and, thus, provides a means of appropriately defining local concentrations. These results confirm previous findings that cluster prevalence increases with decreasing dissipation and that clustered regions have lower temperatures than their dilute counterparts. Surprisingly, however, the results indicate that cluster prevalence, defined by normalized concentration differences between the two regions, decrease monotonically with an increase in overall particle concentration.

DOI: 10.1103/PhysRevE.79.021304 PACS number(s): 45.70.Qj, 47.11.Mn

I. INTRODUCTION

Solids flows are ubiquitous in daily life and industry. The salt and pepper on the dinner table, solid detergents under the sink, and aspirin in the cupboard only hint at the trillion kilograms of granular materials produced each year in the U.S. alone [1]. Indeed, 50% of the products in the chemical industry are solid in form, but this fraction is small compared to the 75% of the raw materials in this industry that are solids [2]. Furthermore, particulate systems in which the gas phase also plays an important role are common in industry, including fluidized beds used in coal gasification, fluid catalytic cracking, production of titania, etc. Accordingly, the investigation of pure granular systems will also provide insight into the granular phase of these multiphase systems. Accordingly, the focus of the current work is on granular systems, and particularly *rapid* flows, in which all momentum is transferred by virtue of binary particle-particle interaction.

Of particular interest within the these particulate systems is the phenomenon known as clustering—the transient formation of regions of high particle concentration. Clusters have been shown to play an important role in the flow characteristics of systems as varied as planetary rings [3–5], high-velocity fluidized beds [6–8] (where interstitial fluid effects are also important), and granular jets [9]. More generally, these transient formations have been observed within homogeneous cooling systems [10–12], simple shear systems [13–16], and Couette systems [17,18], each exhibiting a slightly different form of the inhomogeneity.

The precipitating factor for cluster formation in *granular* systems is particle inelasticity. It should be noted that an additional hydrodynamic driving force arises in *gas-solid* systems [8]. Goldhirsch and Zanetti [10] provided a simple explanation for the relationship between particle inelasticity and cluster formation. A positive density fluctuation results in an increased collision frequency, which in turn decreases the local granular temperature (i.e., kinetic energy of fluctuating particle motion) due to the inelastic interaction between particles. The decreased temperature yields a decreased pressure, providing a gradient that continues to drive particles toward the low-pressure, high-density region. Diffusion of particles out of the cluster serves to balance the driving force toward cluster formation.

Clusters were originally observed in two-dimensional simple shear flows [13], in which they arise with a dominant orientation of +45° from the positive x axis [14,15,19] [see Fig. 1 for axis definitions and Fig. 3(a) for a sample snapshot]. In spite of this general alignment, individual clusters in simple shear have been shown to exhibit a very dynamic nature, consistently forming, rotating, and dissipating [14]. Given this behavior, the primary means of evaluating systems containing such clusters has been a Fourier analysis of a series of snapshots. The resulting Fourier frequency space, from which cluster measurements are made, reflects the com-

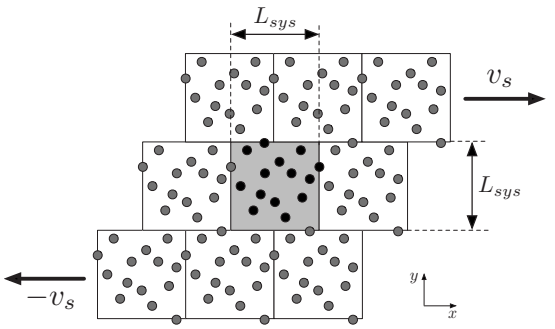

FIG. 1. Simple shear system. Primary computational cell is shaded light gray with black particles. Periodic boundaries are white with gray particles.

*Author to whom correspondence should be addressed: hrenya@colorado.edu

plex spatial orientation of particles and clusters in the system. Physical interpretation of the frequency space is not, however, always straightforward. Hopkins and Louge [13] briefly discuss an ideal case of a two-dimensional sine wave oriented at an angle as an approximation of a clustered system. This simple case yields very clear dominant frequencies in the x and y directions, by which the orientation of the sine wave (i.e., the orientation of the "clusters") and its wavelength (i.e., distance between cluster centers) are easily determined. When particle configurations are more complex [e.g., two-dimensional simple shear flows as displayed in Fig. 3(a)], the complexity of the resulting Fourier analysis follows suit. Features arise throughout the two-dimensional frequency space, reflecting the orientation of clusters and the frequency of their appearance in all directions (e.g., perpendicular to their alignment, parallel to their alignment, etc.). Although dominant frequencies still provide a means of gathering characterization quantities, their relationship to the physical attributes of the system is not as clear.

To build upon previous efforts, the objective of this work is to establish characterizations of clusters that have straightforward physical interpretations, which will be important in future studies of more complex (e.g., polydisperse) systems [20–22]. Here, discrete element models (DEM) will be implemented for the investigation of two-dimensional granular systems under simple shear flow. Two characterizations are developed and implemented for monodisperse systems: a modified form of the radial distribution function $g(r)$ and a concentration and temperature analysis. Both characterization methods provide insight regarding clustered and dilute regions. The data reveal a new feature in the radial distribution function: namely, a long-scale minimum. The associated length scale, which is not present in elastic systems, provides a measure of the average distance between the center of clustered regions (in the direction perpendicular to their known alignment). This quantity is found to be smallest for more inelastic systems at moderate particle concentrations. Furthermore, this length scale is utilized as a basis for a Gaussian filter used to collect concentration and temperature measurements. The ensuing analysis of region concentrations reveals that the disparity between averaged clustered-region and dilute-region concentrations is greatest at moderate particle concentrations, though normalized concentration differences are found to decrease monotonically as the particle concentration increases. Also, an analysis of region-specific temperatures reveals that clustered-region temperatures are lower than dilute-region temperatures over a broad range of systems.

II. COMPUTATIONAL APPROACH

A. Simulation

In the current study, the clustering instability is investigated via two-dimensional, discrete-particle simulations of granular systems. Figure 1 illustrates the two-dimensional ($L_{sys} \times L_{sys}$) computational system, in which simple shear flow is provided by Lees-Edwards boundary conditions [23]. The primary computational cell is indicated by the shaded region. Right and left boundaries are standard periodic boundaries, while upper and lower periodic boundaries move in opposite directions according to a shear velocity (v_s).

TABLE I. System parameter ranges.

Parameter	Symbol	Value (or range)
System size	L_{sys}	$L_{sys}/d >= 90$
Particle size	d	
Volume fraction	ν	0.1–0.5
Restitution coefficient	e	0.6 and 0.8

Particles are treated as frictionless, inelastic, circular disks of constant material density. Due to a lack of body forces, particle trajectories are linear. Each particle is moved forward in time and space according to an event-driven algorithm [24]. Collisions between particles are considered to be binary and instantaneous. A hard-sphere model [24] provides collision resolution based on the conservation of momentum and the dissipation of energy due to particle inelasticity. The resulting post-collision velocities are given by

$$\bar{v}_i^* = \bar{v}_i - \frac{1}{2}(1+e)(\bar{k}\cdot\bar{v}_{ij})\bar{k}, \tag{1}$$

where the asterisk indicates a post-collision quantity, $\bar{k}$ is a unit vector pointing from the center of particle i to the center of particle j, $\bar{v}_{ij}$ is defined as $\bar{v}_i - \bar{v}_j$, and e is the restitution coefficient:

$$e = -\frac{\bar{v}_{ij}^* \cdot \bar{k}}{\bar{v}_{ij} \cdot \bar{k}}. \tag{2}$$

Values of system parameters used in this study are given in Table I. System sizes (L_{sys}/d) have been selected such that clusters are allowed to fully form, per the observations of Liss and Glasser [15] that clustering intensifies with system size until a saturation point is reached. The collection of data from simulations occurs after a statistical steady state is achieved. For the purposes of the current work, the statistical steady state is demarcated by a system time associated with 1000 collisions per particle, after which system stresses have been observed to deviate less than 2% from the average stress values.

After this statistical steady state has been achieved, simulation data are collected in the form of snapshots at intervals of four to five collisions per particle. Each snapshot consists of all particle positions and velocities. From these snapshots, the radial distribution function and analysis of region-specific (clustered and dilute) concentrations and temperatures are obtained, as detailed below.

B. Radial distribution function

The radial distribution function (g) is a measure of the spatial distribution of particles in the system. Specifically, g is defined as the ratio of the *local* particle concentration (at a specified distance r from the center of any given particle) to the *global* (system average) particle concentration. For the purposes of this work, two modifications have been made to

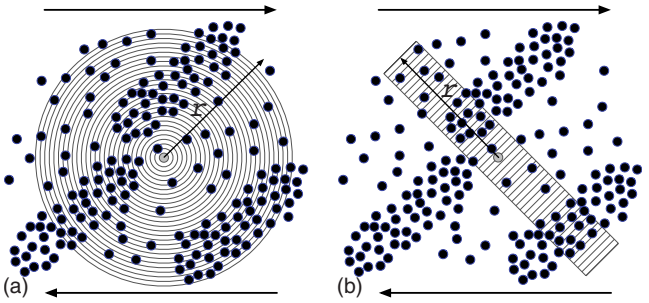

FIG. 2. (Color online) Binning implementation for the radial distribution function in the simple shear flow of inelastic grains. Arrows indicate the direction of shear. (a) Standard implementation of bins in a radial direction from a particle center. (b) Modified implementation of bins in a single direction—i.e., perpendicular to the orientation of clusters.

the standard implementation of the radial distribution function. First, particle concentration is measured based on the area fraction of particles, rather than the number of particles, which is standard for molecular systems. This treatment provides a more general description of the polydisperse particulate systems, which will be considered in a future work. Second, as depicted in Fig. 2, the directional nature of g is modified, so as not to be radial. Instead, g is calculated for a single direction: perpendicular to the known orientation of clusters in simple shear flow (+45° from the positive x axis [13–15,19]). Bins are sized such that they are $0.02d$ in the direction of r and $20d$ particle diameters in the direction perpendicular to r [see Fig. 2(b) for the orientation of r]. The general features of g remain intact for this modified binning method, but the pronunciation of the new long-scale feature associated with these systems is enhanced; this feature will be discussed in the Results and Discussion section.

C. Concentration and temperature measurements by region (clustered or dilute)

Further analysis of clustered systems is made via direct measurement of averaged properties in the clustered and dilute regions. Such measurement requires that the system be depicted as a series of local concentrations rather than a series of discrete particles provided by the simulation snapshots. For this reason, the snapshots of discrete particles, as shown in Fig. 3(a), are first converted to concentration grids. Initially, the grid cells are sized to be ~0.05% of the length of the system (L_{sys}). Given the small grid size, particles are considered to be centered in the grid cell in which the particle center is located, whereby the area of individual particles may be distributed across neighboring grid cells in a straightforward and computationally efficient manner. These small grid cells are then accumulated into larger grid cells with a size of $L_g \approx 0.2d$, which provides accurate calculation of mean velocities and subsequent calculation of fluctuating velocities. Details regarding the selection of the grid sizes, including appropriate sensitivity analyses, are described in [25].

The system is then smoothed as shown in Fig. 3(b) by convolution of the concentration grid with a two-dimensional (2D) Gaussian filter (parameters defining this filter are described in the next section) via the FILTER2 function in OCTAVE (an open source implementation of MATLAB). Finally, grid cells in the smoothed system are classified as clustered or dilute, based on the relationship between their concentration and the average concentration of the system. Concentrations above the average are designated as clustered regions.

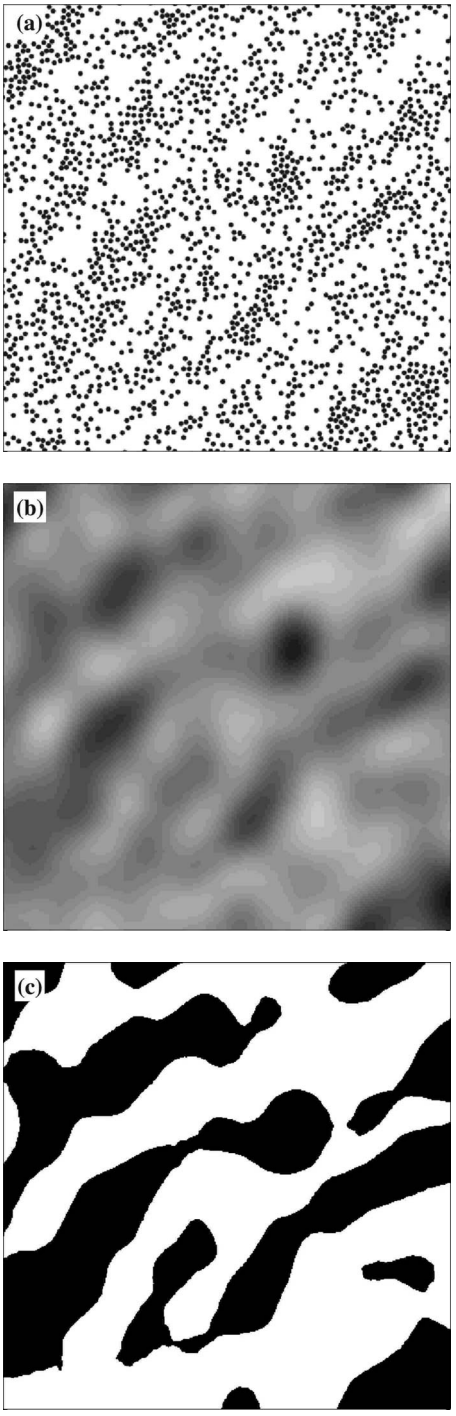

FIG. 3. Example snapshot illustrating (a) discrete particles, (b) the filtered system (white indicates a particle concentration of 0.0 and black indicates a particle concentration of 0.4), and (c) the assignment of clustered (black) and dilute (white) regions. System parameters are as follows: $\nu=0.2$, $e=0.6$, and $L_{sys}/d=90$.

Concentrations below the average are designated as the dilute regions. This classification of clustered and dilute regions is illustrated by Fig. 3(c).

1. Gaussian filter

The Gaussian filter has been designed with the intent of appropriately defining clustered and dilute regions, as described in the following paragraphs. Two considerations in the selection of filter parameters are as follows. First, the sensitivity of measured clustered- and dilute-region properties to the filter parameters should be small. Second, unnecessary computational expense should be avoided. Parameters dictating the filtering process are discussed here. Details regarding their selection and pertinent sensitivity analyses are again left to [25].

As suggested above, the prime consideration in designing the Gaussian filter is whether the filter reflects the *local* properties: namely, those of clustered and dilute regions. If the Gaussian filter is too wide, clustered-region properties will be washed out as a function of the inclusion of the dilute region. If the Gaussian filter is too thin, the filtered system will approximate the system of discrete particles with local concentrations nearing zero and unity. In other words, the filtered concentrations would reflect the presence of individual particles or lack thereof, rather than the concentration of the clustered or dilute *region* under consideration. In this work, the most heavily weighted region of the Gaussian filter will be designed to span the estimated distance between the center of a cluster and the center of a dilute region (i.e., an estimate of the width of each region). This length will be determined based on L (i.e., the location of the long-scale minimum of g), which is discussed in Sec. III A. In particular, since a Gaussian filter will be most heavily weighted within one standard deviation of the mean, the filter is designed such that the length scale L equals two standard deviations (one on either side of the mean), or $L=2\sigma$. The full Gaussian filter incorporates two standard deviations on either side of the mean.

2. Region-specific concentration and temperature measurements

The smoothing process and designation of clustered and dilute region concentrations is performed for a series of snapshots. Based on a sensitivity analysis that is not shown here, the series of snapshots cumulatively contains at least 30×10^6 particles (i.e., the number of snapshots times the number of particles in the system). Concentrations of clustered- and dilute-region grid cells over all snapshots are averaged in order to obtain average concentrations of each region. In addition, the number of clustered- or dilute-region grid cells relative to the total number of grid cells provides an indication of the average area fraction of the system that is clustered or dilute.

Region-specific temperatures are evaluated in a similar manner. For the purposes of assessing granular temperature, however, the classification of clustered and dilute regions is modified in an effort to more clearly differentiate between clustered and dilute regions. Specifically, a buffer of 15% above and below the average concentration of the system is used to distinctly separate the concentrations associated with the clustered and dilute regions. Clustered and dilute regions that are defined in this manner better elucidate the presence of temperature gradients between the two regions without the obfuscation of the ill-defined border between the two regions.

To determine the temperature, the average particle velocity at each point in the shear field is also needed. Average velocities in the x direction are found as a function of y by averaging the velocities of particles whose centers lie within bands of width L_g (grid cell size) at each y value, incorporating all snapshots in the averaging process. After the determination of average particle velocities, snapshots are reevaluated in order to find fluctuating velocities according to the region classifications. Granular temperatures for each region are then calculated via

$$T_X = \frac{1}{2} m \langle v_X' v_X' \rangle, \tag{3}$$

where v' is the fluctuating particle velocity, the subscript X indicates the clustered or dilute region, and $\langle \cdots \rangle$ indicates the average. Temperature ratios (T_{clus}/T_{dil}) are calculated as averages of instantaneous temperature ratios, rather than ratios of averaged temperatures.

III. RESULTS AND DISCUSSION

A. Appearance of a long-scale minimum for inelastic systems

As discussed in Sec. II B, the radial distribution function (g) measures local particle concentrations relative to the average particle concentration, where local is defined as a distance (r) from the center of any given particle. For molecular (elastic) systems in shear flow, the presence of prominent peaks within a few particle diameters is well established. These short-scale features arise as a result of the (in)ability of particles to penetrate one another, which is known as volume exclusion. For the inelastic systems under consideration here, a new feature appears in the radial distribution function profile at longer distances (larger r/d values). This long-scale feature is the focus of the current effort.

Radial distribution functions for both elastic and inelastic systems are provided in Fig. 4, illustrating the similarities and differences at varying restitution coefficients. Prior to the discussion of elastic versus inelastic features, a note should be made regarding the nonzero values below the contact distance ($r/d<1$). Such nonzero values are not observed in the typical (radial) calculation of g. Nevertheless, the modification of the binning scheme from radial to unidirectional (perpendicular to cluster alignment), as discussed in Sec. II B, results in these nonzero values. For example, two particles that are side by side in the direction of cluster alignment are separated by zero distance in the direction perpendicular to cluster alignment, providing local particle concentrations that are greater than zero for $r/d<1$.

Unlike the nonzero values before the distance associated with contact, the remaining features of g are not artifacts of the binning scheme. At the distance associated with contact ($r/d=1$), a peak is observed for both elastic and inelastic

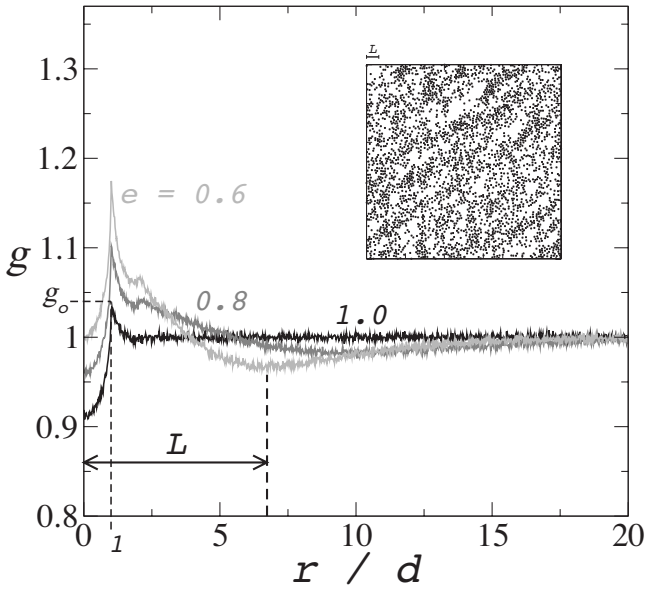

FIG. 4. Radial distribution functions (g) for systems defined by $L_{sys}/d=110$; $\nu=0.2$, and $e=0.6$ (light gray), 0.8 (medium gray), and 1.0 (black). The r/d location of the long-scale minimum provides the length scale (L), as indicated on plot for $e=0.6$. The value of L is also shown to scale by inset system snapshot for $e=0.6$.

systems. This peak decreases with an increasing restitution coefficient. This contact value (g_0) is well known, and the elastic value serves an important role in granular kinetic theory.

Beyond g_0, two other features arise for the *in*elastic systems: a second, smaller peak near g_0 and a more broad, local minimum at distances further from the distance associated with contact. The presence of the second, short-scale peak in the radial distribution functions of clustered systems has been observed by Alam and Luding [22]. Such peaks in the vicinity of the contact distance, however, are also known to arise for elastic systems with higher particle packings. In the case of inelastic systems, the higher *local* packing fraction associated with the clustered regions gives rise to this short-scale feature, which would otherwise not be seen for systems containing lower overall particle concentrations.

The final feature appears *only* for inelastic systems as a broad, local minimum at longer distances (i.e., $r/d > \approx 4$). As the restitution coefficients increases, the location L of this minimum appears at increasing r/d locations, ultimately approaching infinity (i.e., no long-scale minimum) when the restitution coefficient is unity (i.e., an elastic system). The physical meaning of this long-scale minimum can be inferred from the definition of g. Since g is a measure of local particle concentrations, the r/d location of the minimum indicates a distance from any given particle (in the direction perpendicular to known cluster alignment) where another particle would least likely be found. In the context of long-scale concentration inhomogeneities, such as clusters, a minimum located beyond the distances affected by exclusion would be associated with the distance from any given particle where the dilute region would be most likely found.

In an effort to further elucidate the physical meaning the long-scale minimum L, a variety of ideal, one-dimensional

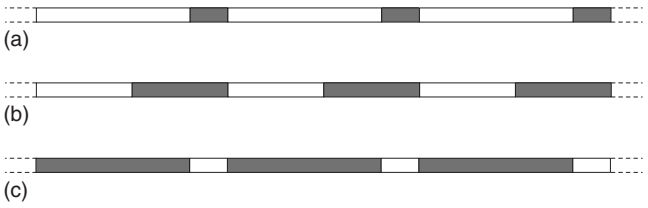

FIG. 5. Sample one-dimensional systems, for which the radial distributions are shown in Fig. 6. Shaded rectangles indicate the clustered region. White rectangles indicate the dilute region. (a) Thin clusters: $f_V=0.2$. (b) Equal cluster- and dilute-region widths: $f_V=0.5$. (c) Thick clusters: $f_V=0.8$.

systems are studied. These ideal, one-dimensional systems are constructed as a series of high-particle-density (clustered) regions separated by low-particle-density (dilute) regions, as illustrated by Fig. 5. Clustered- and dilute-region widths are constant over the system, and each region is populated by a random distribution of particles according to region-specific number densities. Particles are treated as points of infinitesimally small diameter, thereby removing the need to account for exclusion effects. Each one-dimensional system contains 250 clusters ($N_C=250$). Other system attributes are defined based on the fraction of the system that is clustered (f_V), the fraction of the particles that reside in the clustered region (f_P), and the total number of particles in the system (N_P). Systems were investigated with the following parameters: $N_P/N_C=30$, 40, and 50; $f_V=0.2$, 0.5, and 0.8; $f_V \leqslant f_P < 1.0$. Observations noted below are consistent across this parameter space.

Radial distribution functions for these ideal systems are provided in Fig. 6. Long-scale minima appear as troughs with distinct edges. For a scaled comparison, the clustered- and dilute-region widths (W_{clus} and W_{dil}, respectively) are provided as insets below these troughs. As indicated by these insets, the locations of the trough edges are dictated by the clustered- and dilute-region widths. The edge of the trough at the smallest r/d value, where the actual minimum occurs, is consistently associated with the width of the thinnest of the two regions. The corresponding edge at the largest r/d is consistently associated with the widest of the two regions.

The troughlike long-scale minima observed for the ideal systems clearly differ from the smoothed minima observed in simulated systems (Fig. 4). Ideal systems may be modified to better approximate the more varied nature of clusters in 2D simple shear flow systems. In particular, clustered- and dilute-region widths and concentrations in the ideal systems may be randomly varied. Figure 7(a) illustrates the effect of randomly varied region concentrations on the long-scale minimum, while Fig. 7(b) illustrates the effect of randomly varied region widths. The troughlike minima persist when region concentrations are varied [Fig. 7(a)]. On the contrary, the variation of region width tends to smooth the shape of the trough [Fig. 7(b)]. As the extent of the width variation increases from 10% to 30% of the mean width, the distinct edges of the trough minimum give way to a smoothed minimum; the r/d location of this minimum approaches the average width of the clustered and dilute regions (indicated by the vertical dashed line). Practically, the location of this new

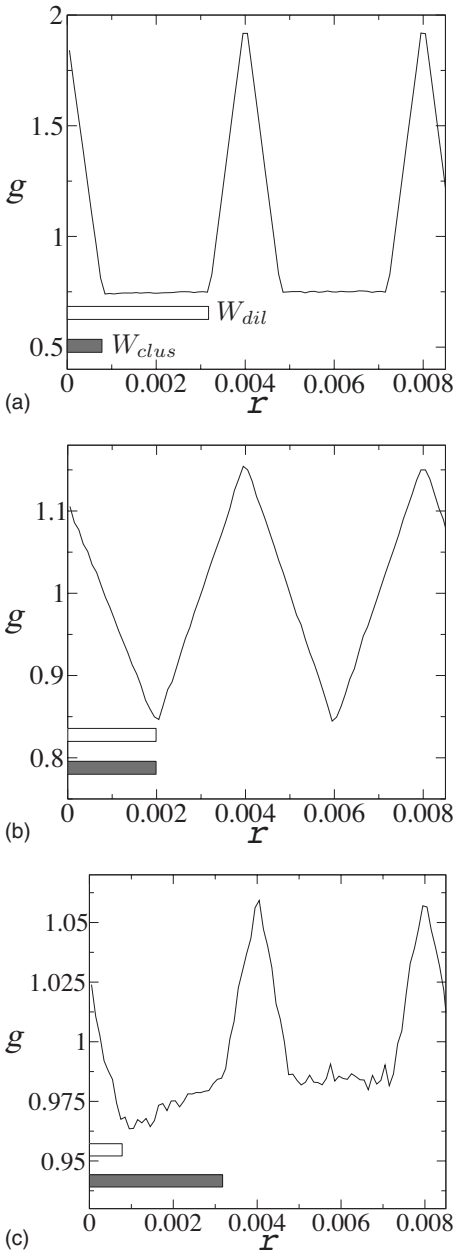

FIG. 6. Sample one-dimensional radial distribution functions for the systems shown in Fig. 5. For all systems, $N_P/N_C=40$. Inset shaded and white rectangles represent clustered- and dilute-region widths, respectively, for comparison with the radial distribution function features. (a) Thin clusters: $f_V=0.2$ and $f_P=0.6$. (b) Equal cluster- and dilute-region widths: $f_V=0.5$ and $f_P=0.7$. (c) Thick clusters: $f_V=0.8$ and $f_P=0.9$.

minimum may be said to tend toward the average distance from the center of a clustered region to the center of a dilute region.

Collectively, observations of the one-dimensional systems indicate that the location and form of the long-scale minimum are determined by clustered- and dilute-region widths. If clustered- and dilute-region widths are consistently sized, the long-scale minimum forms a trough with distinct edges. The actual minimum is located at the width of the thinnest of the two regions. However, if the widths of these regions

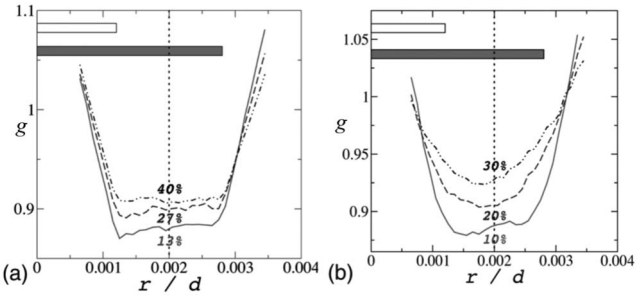

FIG. 7. Close-ups of long-scale minima for one-dimensional systems. Dashed line indicates the average of the clustered- and dilute-region widths—i.e., $(W_{clus}+W_{dil})/2$. Inset shaded and white rectangles represent average clustered- and dilute-region widths, respectively, for comparison with the radial distribution function features. (a) W_{clus} and W_{dil} are held constant throughout the system, while ν_{clus} varies from its mean by by 13%, 27%, and 40%, as displayed in the plot. Other system parameters are defined by $f_V=0.7$, $f_P=0.96$, and $N_P/N_C=40$. (b) ν_{clus} and ν_{dil} are each held constant throughout the system, while W_{clus} varies from its mean by 10%, 20%, and 30%, as displayed in the plot. Other system parameters are defined by $f_V=0.7$, $f_P=0.95$, and $N_P/N_C=40$.

randomly vary about average widths, the long-scale minimum becomes smooth and its location tends toward the average width of the two regions. Given that 2D simple shear flow systems exhibit spatial and temporal variation in the size of clustered and dilute regions, the smooth long-scale minima arising for such systems are expected to tend toward this center-to-center distance. Herein lies a practical physical interpretation of the location of the long-scale minimum, which will be referred to as the radial distribution function length scale L.

B. Cluster characterization measurements in monodisperse, simple shear flows

Having established the methods by which clustered, 2D, simple shear flows may be evaluated, these methods are now applied to monodisperse systems. Length scales (L) will provide insight into the average distance between the clustered and dilute regions. Region analysis will provide insight into the concentrations and temperatures associated with the clustered and dilute regions.

Length scales are provided in Fig. 8 as a function of particle concentration. Data are provided for two restitution coefficients: $e=0.6$ (circles) and 0.8 (squares). As discussed in Secs. II B and III A, the radial distribution function has been designed such that the resulting length scales are dictated by the clustered and dilute region widths in the direction perpendicular to cluster alignment. Specifically, the length scales tend toward the distance between the center of the clustered region and the center of the dilute region. Figure 8 indicates that the shortest length scales arise at low restitution coefficients (consistent with Fig. 4) and moderate particle concentrations.

Qualitatively, the length-scale trends are in agreement with the Fourier-based length-scale trends observed by Hopkins and Louge [13]. The physical interpretation of the

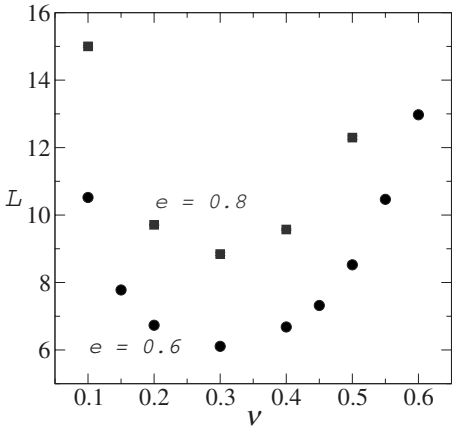

FIG. 8. Variation of length scales with particle concentration. Restitution coefficients of 0.6 and 0.8 are represented by circles and squares, respectively.

Fourier-based length scale is, however, less straightforward than that of the radial distribution function length scale. Whereas the radial distribution function has been designed to reflect clustered- and dilute-region widths in a single direction (perpendicular to the alignment of clusters), the Fourier transform is more ambiguous. The Fourier frequency space, from which the Fourier length scale is derived, reflects all frequencies pertaining to the system. For the purpose of explanation, consider a system in which clusters of particles are represented by the dark squares of a checkerboard. If the bottom and left sides of the checkerboard are aligned along the x and y axes, respectively, and the checkerboard squares (clustered and dilute regions) are stretched in the x direction to form rectangles, then the orientation of individual clusters is parallel to the x axis. However, the cluster-to-cluster orientation (i.e., from the lower left corner to the upper right corner) exhibits a nonzero angle with respect to the x axis. The Fourier frequency space reflects both of these orientations in the 2D frequency space, such that dominant frequencies (and resulting measurement of length scale, cluster orientation, etc.) are not clearly associated with a single physical feature. Therefore, the radial distribution function finds its value in the more straightforward physical interpretation of the resulting length scale.

The region concentration analysis adds to the physical understanding provided by the radial distribution function. Concentration differences between clustered and dilute regions are presented in Fig. 9(a) as a function of particle concentration. Concentration differences are consistently lower at higher restitution coefficients, which follows naturally from the fact that clusters are expected to be less pronounced for more elastic systems. Moreover, concentration differences are greatest at moderate particle concentrations. This behavior is qualitatively consistent with the Fourier observations of Hopkins and Louge [13], who concluded that clusters are most prominent in systems with moderate particle concentrations.

As a different measure of cluster "prevalence," concentration differences may be normalized by the overall particle concentration, as presented in Fig. 9(b). Similar to the non-normalized concentration differences in Fig. 9(a), normalized

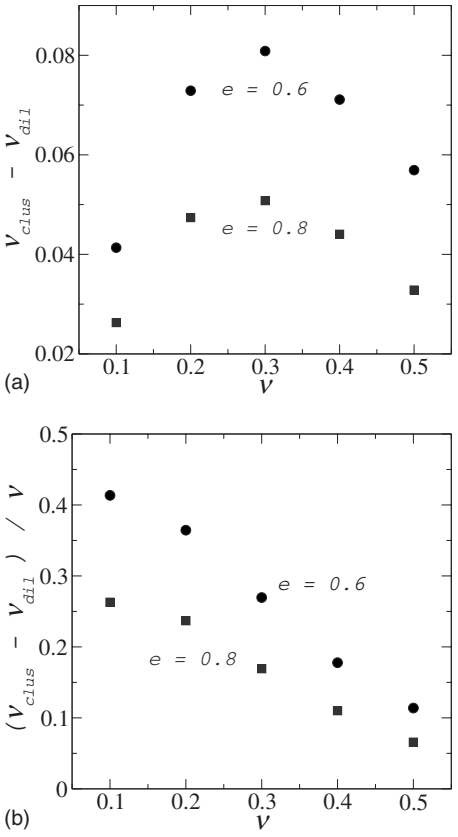

FIG. 9. Concentration differences between clustered and dilute regions over total particle area fraction. Restitution coefficients of 0.6 and 0.8 are represented by circles and squares, respectively. (a) Non-normalized. (b) Normalized by the total particle concentration.

concentration differences increase with increasing restitution coefficient, reflecting the tendency for clusters to be better pronounced for more inelastic systems. With increasing particle concentration, normalized concentration differences decrease. Such behavior is consistent with the fact that systems become more packed at higher concentrations; in the limit of close packing, clusters effectively vanish. However, the behaviors of the normalized and non-normalized concentration differences are qualitatively different at low concentrations, where the non-normalized concentration differences decrease with increasing concentration and the normalized concentration differences increase.

As a final measure of region properties, ratios of clustered-region to dilute-region temperatures (T_{clus}/T_{dil}) are provided in Fig. 10. Temperature ratios that are consistently less than unity indicate that clustered-region temperatures are lower than dilute-region temperatures. Such temperature disparity between the regions reflects the disparity in collision frequency and consequent energy dissipation experienced within the two regions. The higher particle concentrations in the clustered regions provide greater collision frequencies, more energy dissipation, and, thus, lower temperatures. These temperature measurements are consistent with those of Tan and Goldhirsch [14] for a single two-dimensional simple shear flow system and indicate the robustness of this observation. They are also in agreement with temperature observations for granular flow in Couette systems [17,18].

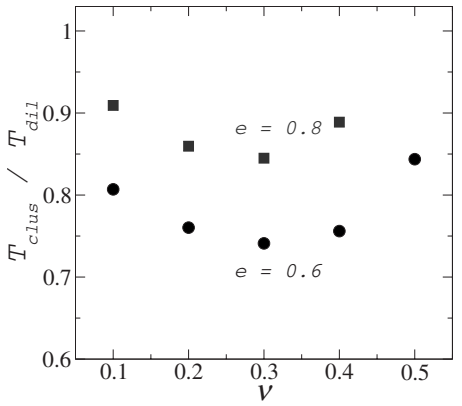

FIG. 10. Ratio of clustered region temperature to dilute region temperature over total particle area fraction. Restitution coefficients of 0.6 and 0.8 are represented by circles and squares, respectively.

C. Interpretation of the depth of the long-scale minimum

While the location (r/d) of the long-scale minimum within g provides a length scale associated with the average distance from the center of a clustered region to the center of a dilute region, the value of g at this minimum also provides physical insight. The "depth" (D) of the minimum is defined as

$$D = 1 - g(L), \tag{4}$$

where g is the radial distribution function and L is the location of the long-scale minimum. Since (i) g is a measure of local concentration relative to the average concentration and (ii) the long-scale minimum is associated with the *dilute* region, $g(L)$ may be approximated as ν_{dil}/ν, thus providing an estimated depth (D_{est}) from Eq. (4) as

$$D_{est} = 1 - \frac{\nu_{dil}}{\nu}, \tag{5}$$

where ν_{dil} is the dilute region concentration and ν is the average concentration of the system.

Depth data are shown in Fig. 11 as a function of overall particle concentration. Depths per Eq. (4) are shown in Fig. 11(a), and estimated depth values per Eq. (5) (incorporating ν_{dil} as calculated by region concentration analysis) are shown in Fig. 11(b). Trends are qualitatively consistent between the two depth values. Depths decrease with increasing restitution coefficient and with increasing total particle concentration. The decrease in depth with increasing restitution coefficient reflects the fact that clusters are less pronounced with more elastic systems. In other words, smaller differences between the average concentration and the dilute-region concentration arise for less clustered, more elastic systems. With respect to the overall particle concentration, the decreasing depths reflect the fact that more densely packed systems do not allow clusters to be strongly pronounced. In the extreme of the close-packed limit, clusters do not exist and the consequent depth would be zero. This monotonic behavior is consistent with the normalized concentration differences displayed in Fig. 9(b).

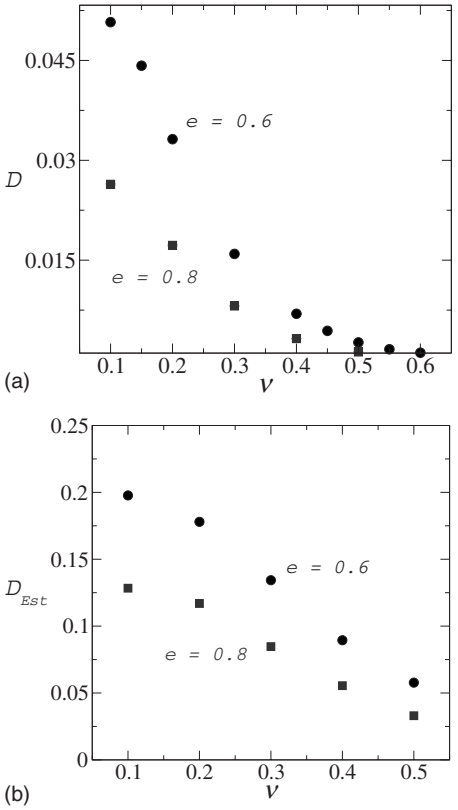

FIG. 11. Radial distribution function depth at the location of the long-scale minimum $[g(L)]$. Restitution coefficients of 0.6 and 0.8 are represented by circles and squares, respectively. (a) Depths as measured based on g. (b) Estimated depths per Eq. (5).

In spite of the qualitative consistency between D and D_{est} trends, strong quantitative differences exist. This lack of quantitative agreement is attributed to the influence of clustered regions on the value of g at the long-scale minimum. Although the location of the long-scale minimum reflects the distance from any particle where the dilute region is most likely to be found, all particles will not see the dilute region at this distance. Therefore, instead of truly reflecting the dilute-region concentration, the depth will reflect a concentration that is greater than the dilute region concentration. The reflection of this higher concentration will yield a depth that is less than that associated purely with the dilute region. In other words, D will be less than D_{est}, as is observed in Fig. 11.

IV. CONCLUDING REMARKS

Two characterization methods—namely, a modified radial distribution function and measurements of concentrations and temperatures of clustered and dilute regions—have been presented for the purpose of further elucidating the characteristics of clustered, two-dimensional simple shear flow. While the current analysis provides results qualitatively consistent with those of previous Fourier analyses, the current approach provides additional quantities plus quantities with cleaner physical interpretation.

First, a new feature in the radial distribution function is shown to exist for inelastic systems. Namely, a long-scale

minimum arises beyond distances associated with particle exclusion. Two measures arise from this new long-scale minimum: a length scale L based on the location of the minimum and a depth D based on the value of g at the minimum. The length scales L are found to represent average separation distances between the center of a clustered region and the center of a dilute region in the direction perpendicular to cluster alignment. For monodisperse systems, these separation distances are smallest (i.e., clusters are most tightly spaced) for systems with moderate particle concentrations and low restitution coefficients. These trends are qualitatively consistent with the Fourier analysis results of Hopkins and Louge [13], though the physical interpretation is more direct in the case of the current characterization. More specifically, the length scale obtained from the complex Fourier frequency space reflects various orientations associated with the clustered system, whereas L is directly linked to intercluster distances. The length scale L finds further use in establishing the width of a Gaussian filter necessary to measure clustered- and dilute-region concentrations. The second radial distribution function measurement—namely, the depth D—provides an additional indication of the difference between the average and dilute-region concentrations, but this measure is unnecessary in light of the directly measured clustered- and dilute-region concentrations.

Directly measured concentration differences between clustered and dilute regions $(\nu_{clus}-\nu_{dil})$ offer clear physical insight into the prevalence of clustering in granular systems. With respect to particle elasticity, concentration differences clearly reveal that clusters are more prevalent in more inelastic systems (i.e., lower restitution coefficients). The cluster prevalence trends with respect to particle concentration are different depending on the normalization of the concentration difference data. Non-normalized data $(\nu_{clus}-\nu_{dil})$ reveal that cluster prevalence is greatest at moderate particle concentrations. This observation is consistent with the Fourier analysis observations of Hopkins and Louge [13], which analyzed non-normalized particle concentrations. Normalized data $[(\nu_{clus}-\nu_{dil})/\nu]$ alternatively reveal that clusters are most prevalent for low concentrations. In particular, the prevalence of clusters diminishes *monotonically* as the system becomes more packed, the extreme of which is a close-packed system in which no clusters would exist. Finally, temperatures of clustered and dilute regions have been measured directly. For a wide range of monodisperse systems, clustered regions have been shown to exhibit lower temperatures than dilute regions.

The presented analysis of monodisperse systems provides a clear foundation for the application to polydisperse systems. Length scales and region-specific measurements may be determined for each unlike species, in addition to the combination. Consequently, the physical interpretation demonstrated for monodisperse systems becomes valuable for the evaluation of each (sub)set of particles, continuing to avoid the complications regarding the physical interpretation of Fourier analysis. Accordingly, the role of each species in the clustered system may be investigated, segregation behavior may be elucidated, and the effect of various particle size distributions on the prevalence of clusters may be determined. Such considerations will be made for both binary and continuous size distribution systems in a future paper.

ACKNOWLEDGMENTS

The authors are grateful to the American Chemical Society Petroleum Research Fund (Grant No. ACS PRF 38065-AC9) for the funding to support this work. R.B.R. also acknowledges support provided by the Department of Education (Grant No. P200A980454).

[1] T. Shinbrot and F. J. Muzzio, Phys. Today **53** (3), 25 (2000).
[2] *Stalics and Kinematics of Granular Materials*, edited by R. M. Nedderman (Cambridge University Press, Cambridge, England, 1992).
[3] *Granular Gases*, edited by T. Poschel and S. Luding (Springer, New York, 2000).
[4] F. Spahn, J. Schmidt, O. Petzschmann, and H. Salo, Icarus **145**, 657 (2000).
[5] P. Tanga, S. J. Weidenschilling, P. Michel, and D. C. Richardson, Astron. Astrophys. **427**, 1105 (2004).
[6] *Multiphase Flow and Fluidization: Continuum and Kinetic Theory Descriptions*, edited by D. Gidaspow (Academic Press, San Diago, 1994).
[7] *Principles of Gas-Solid Flows*, edited by L. S. Fan and C. Zhu (Cambridge University Press, Cambridge, England, 1998).
[8] K. Agrawal, P. N. Loezos, M. Syamlal, and S. Sundaresan, J. Fluid Mech. **445**, 151 (2001).
[9] M. E. Mobius, Phys. Rev. E **74**, 051304 (2006).
[10] I. Goldhirsch and G. Zanetti, Phys. Rev. Lett. **70**, 1619 (1993).
[11] C. Cattuto and U. M. Marconi, Phys. Rev. Lett. **92**, 174502 (2004).
[12] T. Poschel, N. V. Brilliantov, and T. Schwager, J. Phys.: Condens. Matter **17**, S2705 (2005).
[13] M. A. Hopkins and M. Y. Louge, Phys. Fluids A **3**, 47 (1991).
[14] M. L. Tan and I. Goldhirsch, Phys. Fluids **9**, 856 (1997).
[15] E. D. Liss and B. J. Glasser, Powder Technol. **116**, 116 (2001).
[16] M. E. Lasinski, J. S. Curtis, and J. F. Pekny, Phys. Fluids **16**, 265 (2004).
[17] S. L. Conway and B. J. Glasser, Phys. Fluids **16**, 509 (2004).
[18] S. L. Conway, X. Liu, and B. J. Glasser, Chem. Eng. Sci. **61**, 6404 (2006).
[19] P. J. Schmid and H. K. Kytomaa, J. Fluid Mech. **264**, 255 (1994).
[20] S. R. Dahl, R. Clelland, and C. M. Hrenya, Phys. Fluids **14**, 1972 (2002).
[21] S. R. Dahl, R. Clelland, and C. M. Hrenya, Powder Technol. **138**, 7 (2003).
[22] M. Alam and S. Luding, Phys. Fluids **17**, 063303 (2005).
[23] A. W. Lees and S. F. Edwards, J. Phys. C **5**, 1921 (1972).
[24] *Computer Simulation of Liquids*, edited by M. P. Allen and D. J. Tildesley (Oxford University Press, New York, 1989).
[25] R. B. Rice, Ph.D. thesis, University of Colorado at Boulder, 2009.